2017

Hepatocyte ABCA1 Deletion Impairs Liver Insulin Signaling and Lipogenesis

Chia-Chi C. Key

Mingxia Liu

C. Lisa Kurtz

Soonkyu Chung

Elena Boudyguina

See next page for additional authors

Authors
Chia-Chi C. Key, Mingxia Liu, C. Lisa Kurtz, Soonkyu Chung, Elena Boudyguina, Timothy A. Dinh, Alexander Bashore, Peter E. Phelan, Barry I. Freedman, Timothy F. Osborne, Xuewei Zhu, Lijun Ma, Praveen Sethupathy, Sudha B. Biddinger, and John S. Parks

Article

Cell Reports

Hepatocyte ABCA1 Deletion Impairs Liver Insulin Signaling and Lipogenesis

Graphical Abstract

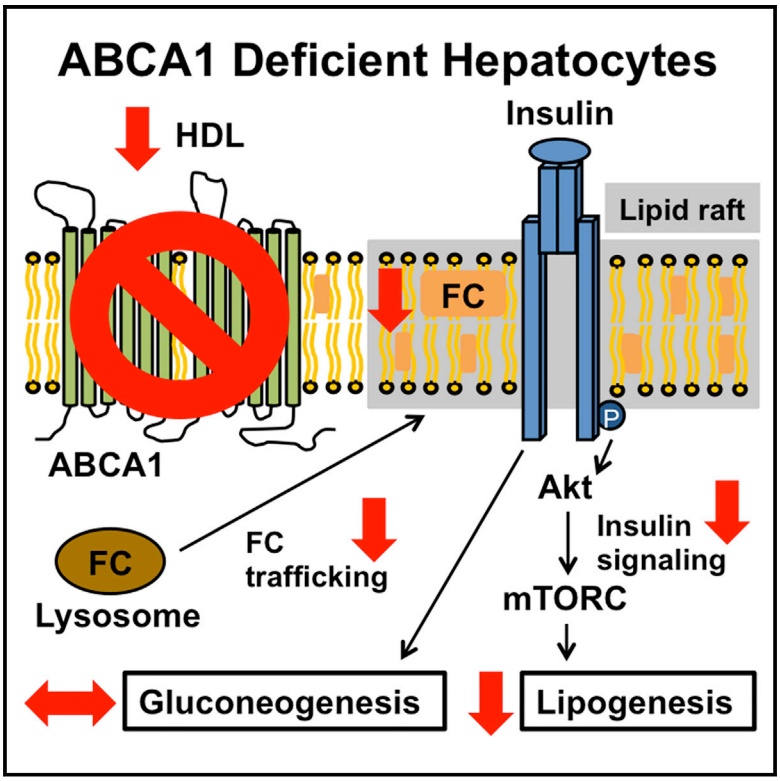

Authors

Chia-Chi C. Key, Mingxia Liu, C. Lisa Kurtz, ..., Praveen Sethupathy, Sudha B. Biddinger, John S. Parks

Correspondence

jparks@wakehealth.edu

In Brief

Key et al. find that deletion of hepatocyte ABCA1 leads to decreased lysosomal free-cholesterol trafficking to the plasma membrane and attenuated cholesterol biosynthesis, resulting in decreased insulin signaling to mTORC1 and attenuated lipogenesis. However, gluconeogenesis remains responsive. Mice lacking hepatocyte ABCA1 are resistant to high-fat-diet-induced hepatosteatosis.

Highlights

- Plasma membrane free cholesterol is decreased in the absence of hepatocyte ABCA1
- Insulin signaling and lipogenesis are attenuated in the absence of hepatocyte ABCA1
- Glucose metabolism is responsive to insulin in the absence of hepatocyte ABCA1
- Hepatocyte-specific *Abca1* deletion protects against high-fat-diet-induced steatosis

Accession Numbers

GSE96093

Key et al., 2017, Cell Reports *19*, 2116–2129
June 6, 2017
http://dx.doi.org/10.1016/j.celrep.2017.05.032

OPEN ACCESS
CellPress

Cell Reports
Article

Hepatocyte ABCA1 Deletion Impairs Liver Insulin Signaling and Lipogenesis

Chia-Chi C. Key,[1] Mingxia Liu,[1] C. Lisa Kurtz,[4] Soonkyu Chung,[6] Elena Boudyguina,[1] Timothy A. Dinh,[4,5] Alexander Bashore,[1] Peter E. Phelan,[7] Barry I. Freedman,[2] Timothy F. Osborne,[7] Xuewei Zhu,[1] Lijun Ma,[2] Praveen Sethupathy,[4,5,9] Sudha B. Biddinger,[8] and John S. Parks[1,3,10,*]

[1]Section on Molecular Medicine, Department of Internal Medicine
[2]Section on Nephrology, Department of Internal Medicine
[3]Department of Biochemistry
Wake Forest School of Medicine, Winston-Salem, NC 27157, USA
[4]Department of Genetics
[5]Curriculum in Genetics and Molecular Biology
University of North Carolina at Chapel Hill, Chapel Hill, NC 27599, USA
[6]Department of Nutrition and Health Sciences, University of Nebraska, Lincoln, NE 68588, USA
[7]Integrative Metabolism Program, Sanford Burnham Prebys Medical Discovery Institute, Orlando, FL 32827, USA
[8]Division of Endocrinology, Boston Children's Hospital, Harvard Medical School, Boston, MA 02062, USA
[9]Present address: Department of Biomedical Sciences, College of Veterinary Medicine, Cornell University, Ithaca, NY 14853, USA
[10]Lead Contact
*Correspondence: jparks@wakehealth.edu
http://dx.doi.org/10.1016/j.celrep.2017.05.032

SUMMARY

Plasma membrane (PM) free cholesterol (FC) is emerging as an important modulator of signal transduction. Here, we show that hepatocyte-specific knockout (HSKO) of the cellular FC exporter, ATP-binding cassette transporter A1 (ABCA1), leads to decreased PM FC content and defective trafficking of lysosomal FC to the PM. Compared with controls, chow-fed HSKO mice had reduced hepatic (1) insulin-stimulated Akt phosphorylation, (2) activation of the lipogenic transcription factor Sterol Regulatory Element Binding Protein (SREBP)-1c, and (3) lipogenic gene expression. Consequently, Western-type diet-fed HSKO mice were protected from steatosis. Surprisingly, HSKO mice had intact glucose metabolism; they showed normal gluconeogenic gene suppression in response to re-feeding and normal glucose and insulin tolerance. We conclude that: (1) ABCA1 maintains optimal hepatocyte PM FC, through intracellular FC trafficking, for efficient insulin signaling; and (2) hepatocyte ABCA1 deletion produces a form of selective insulin resistance so that lipogenesis is suppressed but glucose metabolism remains normal.

INTRODUCTION

On binding to its receptor, insulin stimulates signaling events that, ultimately, profoundly change metabolism (Biddinger and Kahn, 2006). One such change is the stimulation of hepatic lipogenesis (Horton et al., 1998). Defective insulin signaling occurs in obesity, diabetes, and metabolic syndrome (Leavens and Birnbaum, 2011; Saltiel and Kahn, 2001). Changes in plasma membrane (PM) free cholesterol (FC) content and phospholipid species (i.e., fatty acyl and head group) modulate the signaling of multiple receptors (Simons and Toomre, 2000), suggesting that PM FC content could also regulate insulin signaling. In support of this notion, excess PM FC in Niemann-Pick C1 knockout hepatocytes, or chemical depletion of PM FC (i.e., too little PM FC) in wild-type hepatocytes, blunted insulin receptor autophosphorylation, hinting that optimal PM FC is necessary for efficient insulin receptor activation (Vainio et al., 2002, 2005).

ATP binding cassette transporter A1 (ABCA1) effluxes FC and phospholipid (PL) across the PM to combine with apolipoproteins (i.e., apoA–I), forming nascent high-density lipoproteins (HDLs) (Oram and Vaughan, 2006). While a role for ABCA1 in bulk cellular FC export is well recognized (Oram and Vaughan, 2006), recent studies suggest that ABCA1 modifies PM lipid composition, which results in altered signaling via PM receptors. For example, myeloid-specific deletion of *Abca1* results in macrophages with increased PM FC and lipid raft content (Zhu et al., 2008, 2010). These macrophages are hyper-responsive to pathogen-associated molecular pattern molecules due to increased localization of Toll-like receptors and adaptor proteins in lipid rafts (Ito et al., 2015; Zhu et al., 2012), which increases macrophage secretion of proinflammatory cytokines (Zhu et al., 2008), chemotaxis in vitro and in vivo, and clearance of live bacteria from circulation (Zhu et al., 2012). Increased PM FC in hematopoietic stem and multipotential progenitor cells augments signaling through the interleukin-3 (IL-3) receptor and cell proliferation (Murphy et al., 2011; Yvan-Charvet et al., 2010). Recently, ABCA1 was implicated in modifying membrane lipid composition and multiple signaling activities in response to cell crowding (Frechin et al., 2015).

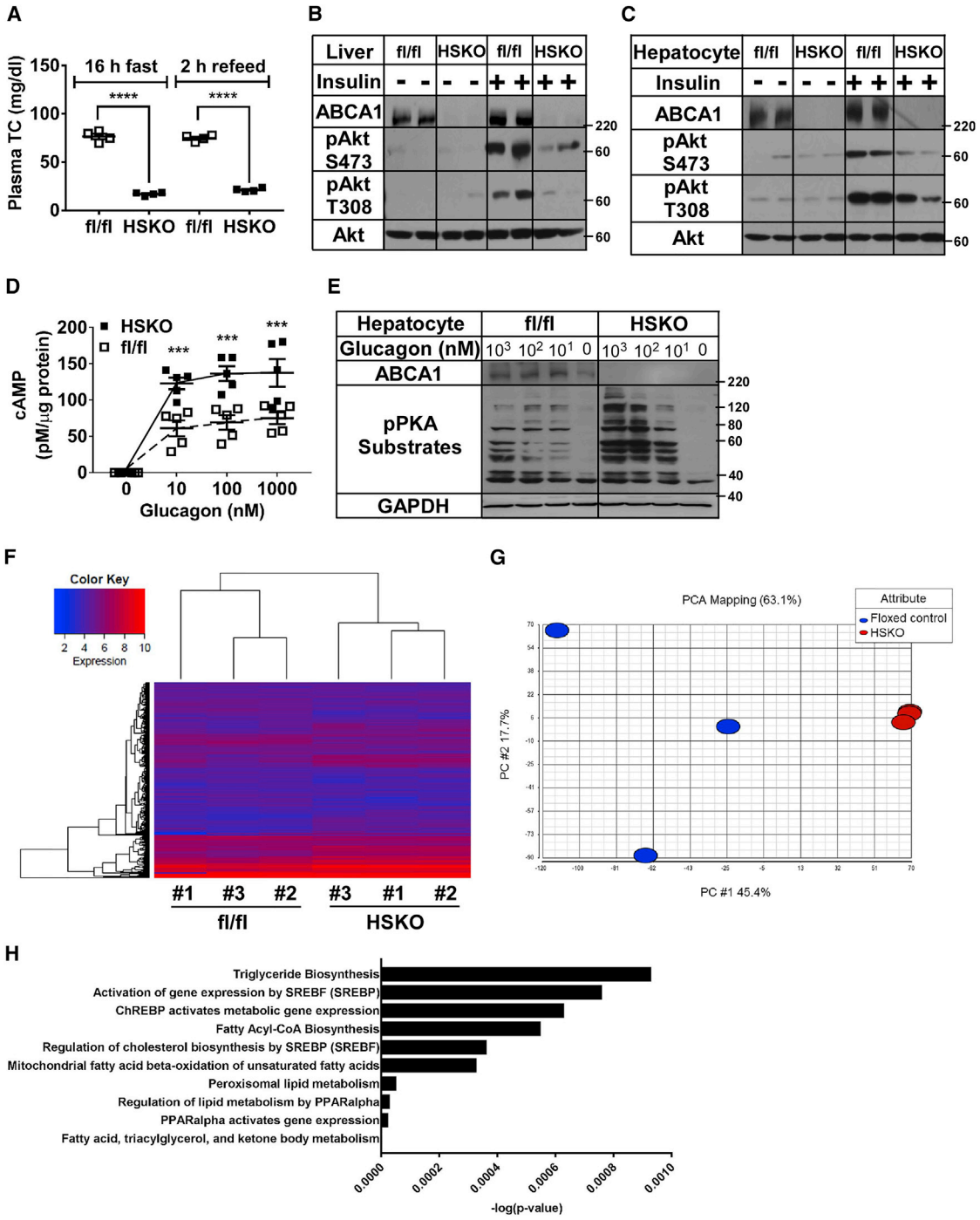

Figure 1. Hepatic Insulin and Glucagon Signaling and Transcriptome Profile

(A) Mice (n = 4 per genotype) were fasted and then fed chow for 2 hr. Blood samples were obtained and isolated plasma used to measure total cholesterol (TC) concentration.

(B) Western blot of liver Akt activation.

(C) Western blot of hepatocyte Akt activation.

(D and E) Glucagon signaling in primary hepatocytes. (D) Cyclic AMP (cAMP) levels measured with ELISA. (E) PKA phosphorylation substrates (pPKA substrates) were determined by western blotting.

(F and G) Chow-fed mice were fasted for 4 hr, and livers were harvested for RNA-seq (n = 3 per genotype). (F) Heatmap and clustering of 3,000 most variably expressed genes in the normalized RNA-seq dataset. (G) PCA analysis.

(legend continued on next page)

Several lines of indirect evidence suggest that ABCA1 may be involved in insulin signaling. Chow-fed *Abca1* global KO mice develop hyperglycemia by 4 months of age, and pancreatic β cell-specific deletion of *Abca1* results in islet cell FC accumulation and defective insulin release, leading to hyperglycemia (Brunham et al., 2007). Chow-fed hepatocyte-specific *Abca1* knockout (HSKO) mice show phenotypic lipid changes similar to those in type 2 diabetes and metabolic syndrome (Adiels et al., 2005), including elevated non-fasting plasma triglyceride (TG) levels from hepatic overproduction of large TG-enriched VLDL1 (very low-density lipoprotein 1) particles and low plasma HDL concentrations (Chung et al., 2010). Chow-fed HSKO mice also have diminished phosphoinositide 3-kinase (PI3K) and Akt activation with fasting and refeeding or acute insulin injection (Chung et al., 2010). Chow-fed female HSKO mice have impaired glucose tolerance but unchanged insulin sensitivity (de Haan et al., 2014a). Mounting evidence suggests that ABCA1 SNPs are associated with type 2 diabetes and metabolic syndrome in humans (Daimon et al., 2005; Porchay et al., 2006; Villarreal-Molina et al., 2007, 2008). Nonetheless, a direct role of ABCA1 in insulin receptor signaling has not been reported.

Here, we sought to determine whether hepatocyte ABCA1 expression affects PM lipid composition, insulin signaling, and lipogenesis. Although liver FC and CE content are similar in chow-fed HSKO and control mice (Chung et al., 2010), we hypothesized that hepatocyte PM cholesterol is elevated in HSKO mice, resulting in blunted insulin signaling in livers of chow-fed HSKO mice versus control mice. This hypothesis was based on reports that myeloid-specific deletion of ABCA1 results in macrophages with increased PM FC and lipid raft content (Zhu et al., 2008, 2010), and optimal PM FC content is necessary for hepatocyte insulin signaling (Vainio et al., 2002, 2005).

RESULTS

Hepatocyte-Specific *Abca1* Deletion Modifies Hepatic Insulin and Glucagon Signaling in Chow-Fed Mice

Chow-fed HSKO mice had total plasma cholesterol concentrations 72%–78% lower ($p < 0.0001$) than in *Abca1*$^{floxed/floxed}$ (fl/fl) control mice (Figure 1A), as previously reported (Chung et al., 2010; Timmins et al., 2005). Although body weight and food intake decreased and blood glucose and plasma insulin increased in chow-fed HSKO mice, the systemic metabolic phenotype (Figures S1A–S1Q) was not statistically different from that of fl/fl mice.

We reported earlier that chow-fed HSKO mice had reduced hepatic phosphorylation of Akt serine residue 473 (S473) and PI3K p85 compared to controls, suggesting hepatic insulin resistance in HSKO mice (Chung et al., 2010). Complete Akt activation requires phosphorylation at S473 and threonine residue 308 (T308) (Cheng and White, 2012; Wu and Williams, 2012). Here, we observed that both phosphorylated sites were decreased in the liver (Figure 1B) and hepatocytes (Figure 1C) of chow-fed HSKO versus control mice.

We also investigated whether hepatocyte ABCA1 deletion also affected glucagon signaling, which activates adenylate cyclase, resulting in increased cyclic AMP (cAMP) concentration and cAMP-induced protein kinase A (PKA) activity (Campbell and Drucker, 2015). Incubation of hepatocytes from chow-fed HSKO mice with glucagon led to a doubling of cAMP levels (Figure 1D; $p < 0.001$) and substrates of PKA phosphorylation, compared to hepatocytes from fl/fl control mice (Figure 1E).

Hepatocyte-Specific *Abca1* Deletion Impairs Hepatic De Novo Lipogenesis

We applied an unbiased RNA-sequencing (RNA-seq) approach to identify differential gene signatures in livers of chow-fed HSKO versus fl/fl control mice. We obtained an average of ~100 million paired-end reads per sample, ~85% of which mapped uniquely to the mouse genome. Clustering analysis using the 3,000 most variably expressed genes correctly distinguished the fl/fl and HSKO mice (Figure 1F). This clustering was confirmed (1) by analyzing the 3,000 most highly expressed genes (Figure S2A) and the 10,000 most variable or most highly expressed genes (data not shown) and (2) by principal-component analysis (PCA) (Figure 1G). The mRNA expression levels of 906 genes were significantly altered in livers of HSKO versus fl/fl control mice, including 226 downregulated (<2 fold) and 680 upregulated (>2-fold) genes (both unadjusted $p = 0.05$; Tables S1 and S2). As expected, *Abca1* mRNA was among the most significantly downregulated (~90% loss, unadjusted $p = 3.2E{-}05$; Table S1). Using the Reactome 2016 database, the 226 downregulated genes were most significantly overrepresented in pathways related to lipogenesis, including fatty acyl-coenzyme A (CoA) synthesis ($p = 0.0006$) and TG biosynthesis ($p = 0.0009$) (Figure 1H; Table S3). Moreover, using the BioCarta 2016 resource, sterol regulatory element binding protein (SREBP) control of lipid synthesis is one of only two significantly enriched pathways ($p = 0.01$) among downregulated genes (Table S3). We verified these findings by real-time qRT-PCR for genes that encode key enzymes in lipogenesis (Figure S2B).

Primary hepatocytes were isolated from chow-fed mice, and rates of TG, FC, PL, and cholesteryl ester (CE) synthesis were determined by measuring the incorporation of [^{14}C]-acetic acid (i.e., de novo lipogenesis) and [^{3}H]-oleic acid (TG formation by fatty acid [FA] esterification) into hepatocyte lipids. TG (Figure 2A), FC (Figure 2B), PL (Figure 2C), and CE (Figure 2D) synthesis from [^{14}C]-acetic acid was significantly decreased in hepatocytes from HSKO versus fl/fl control mice, supporting the RNA-seq results. TG (Figure 2E), but not PL (Figure 2F) and CE (Figure 2G), formation by [^{3}H]-oleic acid esterification was significantly reduced in HSKO hepatocytes, suggesting that the primary effect of hepatocyte ABCA1 deletion was on de novo lipogenesis and somewhat on FA uptake and esterification into TG.

(H) Pathway analysis of RNA-seq dataset using the Reactome 2016 database.
In (A)–(E), results are representative of two to three separate experiments.
*$p < 0.05$; **$p < 0.01$; ***$p < 0.001$; and ***$p < 0.0001$. All results are mean ± SEM.
See also Figures S1 and S2.

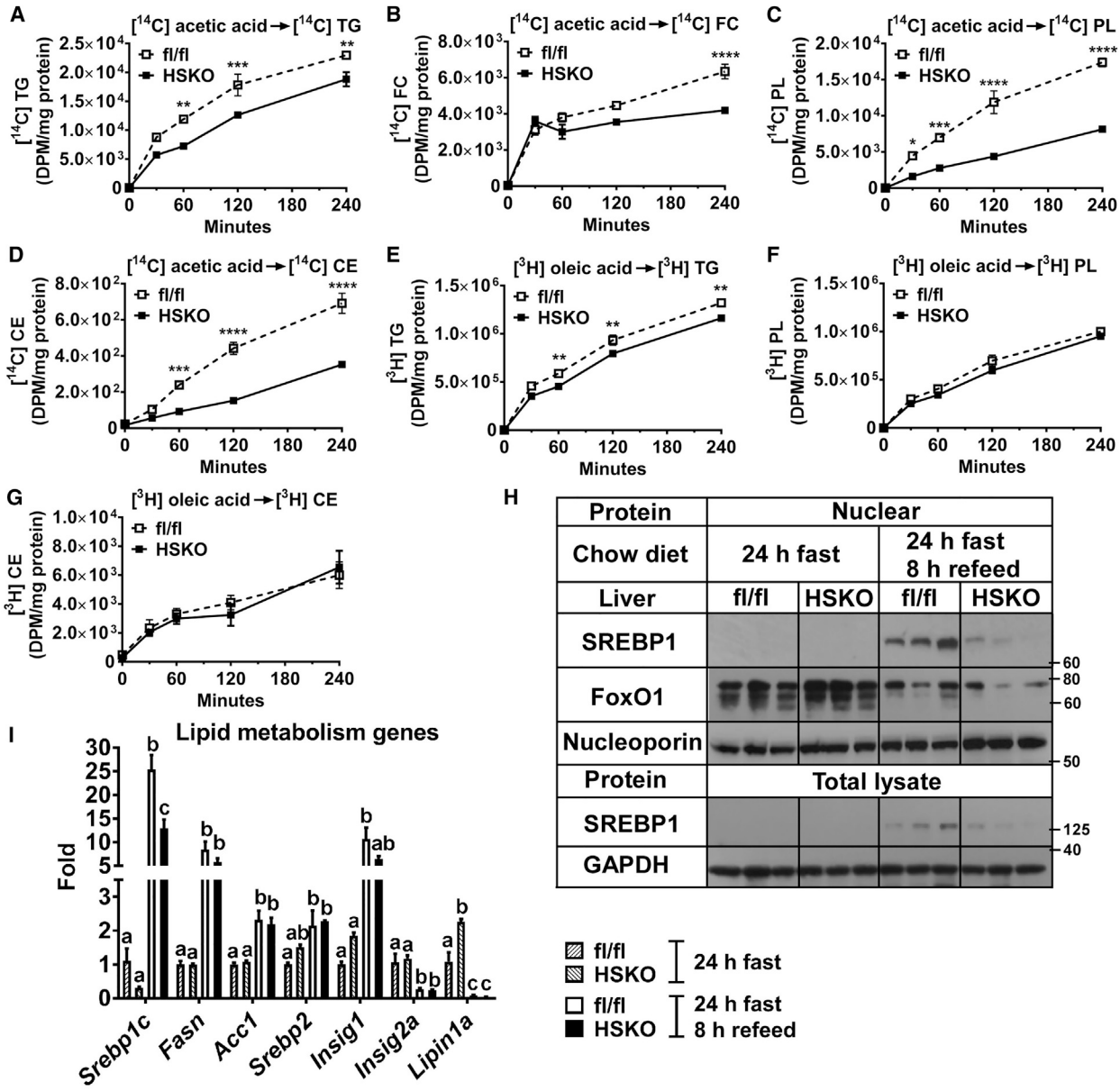

(legend on next page)

Since insulin signaling was blunted and lipogenesis was decreased in HSKO hepatocytes, compared to fl/fl hepatocytes, we examined expression and proteolytic processing of SREBP1c, the master regulator of de novo lipogenesis (Goldstein and Brown, 2015). Mice were subjected to a 24-hr fast followed by 8-hr refeeding of a high-carbohydrate chow diet, which results in robust expression and proteolytic processing of SREBP1c as insulin levels rise during the refeeding period (Engelking et al., 2004; Haas et al., 2012; Horton et al., 1998). After a 24-hr fast, minimal full-length or processed SREBP1c was observed (Figure 2H) due to low insulin levels. However, after 8 hr of refeeding when insulin is high, full-length SREBP1c and nuclear-processed SREBP1c were markedly reduced in HSKO versus fl/fl liver (Figure 2H). As anticipated (Yabe et al., 2003), after 8 hr of refeeding, *Srebp1c* (25-fold, $p < 0.0001$), FA synthase (*Fasn*; 8-fold, $p < 0.01$), acetyl-CoA carboxylase 1 (*Acc1*; 2-fold, $p < 0.01$), *Srebp2* (2-fold, $p < 0.05$), and *Insig1* (11-fold, $p < 0.01$) hepatic mRNA increased; and *Insig2a* and *Lipin1a* decreased (Figure 2I) in both genotypes. However, HSKO mouse liver had significantly lower mRNA for *Srebp1c* after the 8-hr refeeding period and a trend toward less *Fasn* and *Insig1* mRNA versus refed fl/fl livers (Figure 2I).

We also examined signaling proximal and distal to the mechanistic target of rapamycin C1 (mTORC1), a bifurcation point between insulin-stimulated lipogenesis and gluconeogenesis (Li et al., 2010), using insulin-stimulated primary hepatocytes isolated from chow-fed mice. We observed significantly decreased phosphorylation of tuberous sclerosis complex 2 (TSC2), ribosomal protein S6 kinase 1 (S6K1), eukaryotic initiation factor 4E-binding protein 1 (4E-BP1), and glycogen synthase 3β (GSK3β), but not proline-rich Akt substrate of 40 kDa (PRAS40), in hepatocytes from chow-fed HSKO versus fl/fl mice (Figures 2J and S2C), supporting decreased mTORC activation and de novo lipogenesis in HSKO hepatocytes.

Hepatocyte-Specific *Abca1* Deletion Does Not Impair Hepatic Glucose Metabolism

As anticipated (Yabe et al., 2003), 8 hr of refeeding after a 24-hr fast decreased mRNA abundance for the gluconeogenic genes phosphoenolpyruvate carboxykinase (*Pepck*; $p < 0.01$), glucose-6-phosphatase (*G6pc*; $p = 0.2$), insulin receptor substrate 2 (*Irs2*; $p = 0.1$), and insulin-like growth-factor-binding protein 1 (*Igfbp1*; $p < 0.01$), and it increased expression of the glycolysis gene glucokinase (*Gck*; $p = 0.001$) in livers of fl/fl control mice (Figure 2K). HSKO mouse liver had higher mRNA abundance for *G6pc* ($p < 0.05$) and *Igfbp1* ($p < 0.0001$) after the 24-hr fast and lower *Pepck*, *G6pc*, *Irs2*, and *Igfbp1* mRNA versus refed fl/fl livers (Figure 2K). In agreement with results in Figure 2K, we observed increased nuclear FoxO1; on refeeding, nuclear FoxO1 appeared slightly lower in HSKO livers versus fl/fl livers (Figure 2H). Overall, these results show that FoxO1 signaling is unimpaired in fasted-refed HSKO versus fl/fl mice.

Hepatocyte-Specific *Abca1* Deletion Stimulates Hepatic FA Oxidation

Since our RNA-seq results suggested that FA oxidation pathways were downregulated in HSKO liver (Table S3), we measured rates of FA uptake and oxidation of [^{14}C]-palmitic acid into [^{14}C]-CO_2 and [^{14}C]-acid-soluble metabolites (ASMs). FA oxidation was increased in hepatocytes from chow-fed HSKO versus fl/fl mice (Figures S2D and S2E), whereas FA uptake was similar (Figure S2F).

Hepatocyte-Specific *Abca1* Deletion Improves Metabolic Phenotype of WTD-Fed Mice

We challenged chow-fed HSKO mice with a Western-type diet (WTD), which decreased their weight versus fl/fl mice (Figure 3A). WTD-fed HSKO mice had significantly increased oxygen consumption (Figure 3B) and energy expenditure (Figure 3C), without changes in food intake, physical activity, or respiratory exchange ratio (Figures S3A–S3C). Similar to our previous reports (Chung et al., 2010; Timmins et al., 2005), HSKO mice had reduced plasma LDL (low-density lipoprotein) cholesterol and HDL cholesterol concentrations, compared to fl/fl mice on both chow and WTD (Figure S3D). Other measures of a systemic metabolic phenotype between WTD-fed HSKO and fl/fl mice were similar (Figures S3E–S3L). However, liver TG (Figures 3D and 3E) and FC (Figure 3F) levels were decreased 70% ($p < 0.0001$) and 20% ($p < 0.01$), respectively, in WTD-fed HSKO versus fl/fl control mice. TG (Figure 3G) and FC (Figure 3H) levels were also decreased 70% ($p < 0.0001$) and 30% ($p < 0.01$), respectively, in hepatocytes from WTD-fed HSKO versus fl/fl control mice.

To determine the mechanism for reduced hepatosteatosis in WTD-fed HSKO mice, we examined several pathways that influence hepatic TG content. Incorporation of [^{14}C]-acetic acid into TG (Figure 4A) and PL (Figure 4B) was significantly decreased in primary hepatocytes isolated from WTD-fed HSKO versus fl/fl control mice, demonstrating decreased hepatic de novo lipogenesis. Newly synthesized FC (Figure 4C) from [^{14}C]-acetic acid was similar between genotypes, likely due to feedback inhibition by cholesterol in the WTD. [^{3}H]-oleic acid esterification into hepatocyte TG (Figure 4D) and PL (Figure 4E) was also reduced in hepatocytes from WTD-fed HSKO mice, similar to results with

Figure 2. Lipid Metabolism in Hepatocytes from Chow-Fed Mice

(A–G) Primary hepatocytes were incubated with the indicated radiolabels and newly synthesized TG (A and E), FC (B), PL (C and F), and CE (D and G) measured (n = 3 per time point).

(H and I) Mice (n = 3 per genotype) underwent fasting and refeeding; nuclear and total liver protein (H) and total RNA (I) from mouse livers were subjected to western blotting and real-time PCR quantification, respectively.

(J) Primary hepatocytes were treated with saline (−) or insulin (+) for 2 min to examine pTSC2, TSC2, pPRAS40, and PRAS40 or 5 min to examine pS6K1, S6K1, pGSK3β, Gsk3β, p4E-BP1, and 4E-BP1 protein expression.

(K) Real-time PCR quantification of glucose metabolism genes. Same experimental conditions and animals as in (I).

Results are representative of two to three separate experiments. *$p < 0.05$; **$p < 0.01$; ***$p < 0.001$; and ****$p < 0.0001$; for multiple comparisons, different lowercase letters denote significant differences, $p < 0.05$. All results are mean ± SEM.

See also Figure S2.

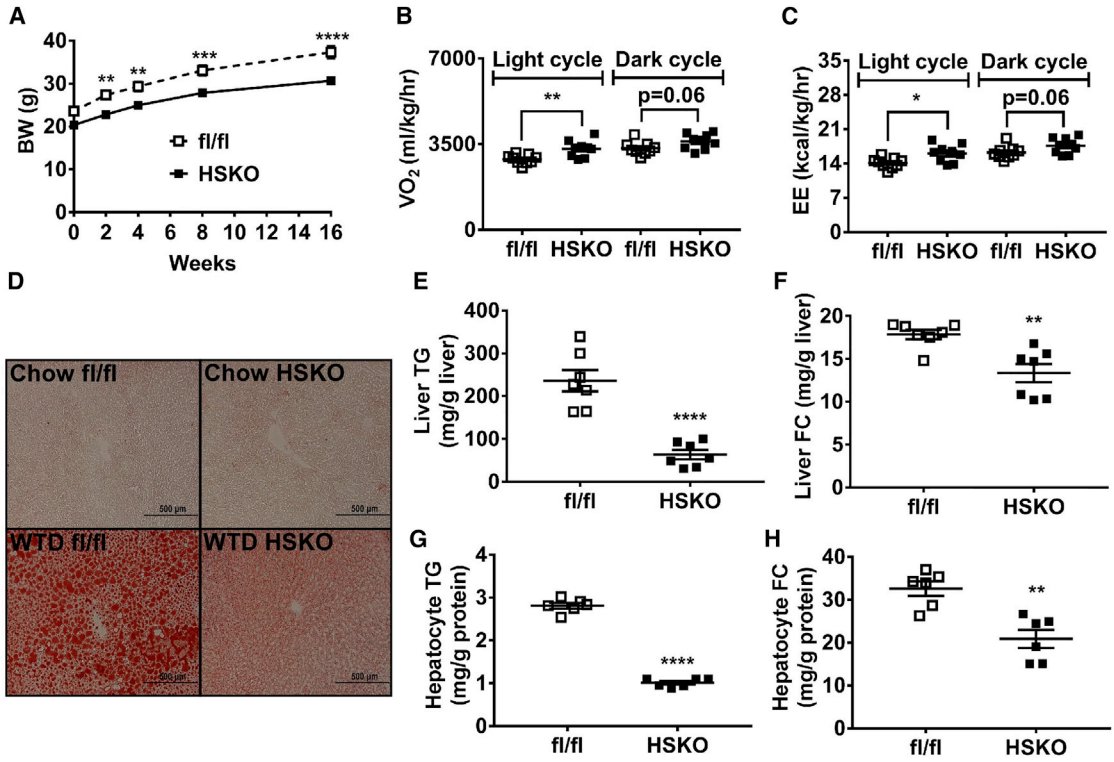

Figure 3. Metabolic Phenotype of WTD-Fed Mice

Male mice were fed a WTD for 16–24 weeks.

(A) Body weight (BW); n = 9.

(B) Oxygen consumption rates (VO_2) in milliliters per kilogram per hour (mL/kg/hr).

(C) Energy expenditure (EE) in kilocalories per kilogram per hour (kcal/kg/hr).

(D) Oil red O staining of representative liver sections from 16-week WTD-fed mice.

(E–H) Liver TG (E) and FC (F) and hepatocyte TG (G) and FC (H) from WTD-fed mice. Data are representative of two to three separate experiments.

*p < 0.05; **p < 0.01; ***p < 0.001; and ****p < 0.0001. All results are mean ± SEM.

See also Figure S3.

[^{14}C]-acetic acid. WTD-fed HSKO mice, versus fl/fl control mice, also had decreased hepatocyte [^{14}C]-palmitic acid uptake (Figure 4F), decreased liver CD36/FA translocase mRNA levels (Figure 4G; 50%, p < 0.001), and reduced liver PM and cytosolic CD36/FA translocase protein expression (Figure 4H); however, hepatocyte FA oxidation was similar (Figures S4A and S4B), as was hepatic gene expression of peroxisome-proliferator-activated receptor α (*Ppar*α), carnitine palmitoyltransferase 1 (*Cpt1*), and *Acc2* (Figure S4C). Lastly, in vivo secretion of newly synthesized VLDL-TG from [^{3}H]-oleic acid (Figures S4D and S4E) was similar for WTD-fed wild-type (WT) and HSKO mice. Thus, attenuated diet-induced hepatosteatosis in HSKO mice was most likely due to decreased hepatic de novo lipogenesis and FA uptake.

Impaired Hepatic Insulin Signaling in HSKO Liver Is Associated with Decreased PM FC and Increased Hepatic Lyso-PL Levels

Portal vein insulin injection in WTD-fed HSKO mice resulted in decreased hepatic insulin-stimulated Akt S473 and T308 phosphorylation versus controls (Figure 5A). However, white adipose tissue (Figure S5A) and skeletal muscle (Figure S5B) insulin signaling was similar for both genotypes, suggesting that insulin signaling was selectively impaired in hepatocytes lacking ABCA1 expression. We also isolated liver PM from mice with a portal vein insulin injection. WTD-fed HSKO liver had decreased PM insulin receptor phosphorylation, but there was no change in insulin receptor β protein expression versus that in fl/fl control mice, suggesting decreased activation of hepatic insulin receptor in WTD-fed HSKO mice (Figure 5B).

We hypothesized that hepatocyte-specific ABCA1 deletion increased PM FC content, leading to impaired insulin signaling. Primary hepatocytes from chow- or WTD-fed mice were used to isolate PM fractions, which were then lipid extracted to measure FC. The PM fraction (enriched in Na^+/K^+ ATPase) isolated from chow-fed mouse hepatocytes was relatively free of calnexin and perilipin 2 (Figure 5C). We also examined the abundance of PM flotillin 1, a protein associated with caveolar lipid rafts (Bickel, 2002; Bickel et al., 1997). Hepatocyte PM flotillin 1 (Figure 5C) and FC (Figure 5D; ~60%, p < 0.05) content were significantly decreased in chow-fed HSKO versus control mice. As with our chemical measurement of PM FC, filipin staining was decreased in the PM region of chow HSKO versus fl/fl hepatocytes (Figure S5C).

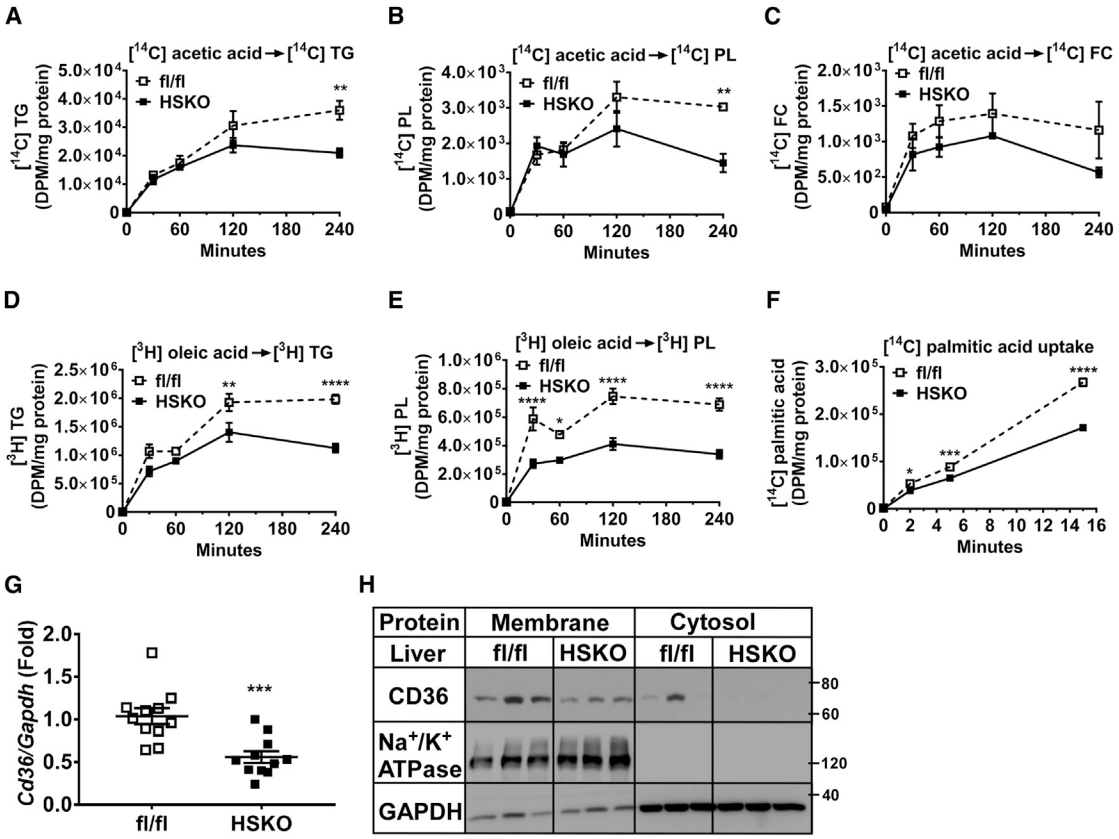

Figure 4. Lipid Metabolism in Primary Hepatocytes from WTD-Fed Mice

(A–E) Primary hepatocytes from WTD-fed mice (n = 2 per genotype) were incubated with the indicated radiolabels and newly synthesized ^{14}C-triglyceride (TG) (A), ^{14}C-phospholipid (PL) (B), ^{14}C-free cholesterol (FC) (C), ^{3}H-TG (D), and ^{3}H-PL (E) were measured (n = 3 per time point).

(F) FA uptake by primary hepatocytes was measured as in Figure 2 (n = 3 per time point); two-way ANOVA with Bonferroni's multiple comparison test.

(G) *Cd36* expression by real-time PCR.

(H) Hepatic CD36, Na^+/K^+ ATPase, and GAPDH protein expression.

Results are representative of two to three separate experiments. *$p < 0.05$; **$p < 0.01$; ***$p < 0.001$; and ****$p < 0.0001$. All results are mean ± SEM. DPM, disintegrations per minute.

See also Figure S4.

HSKO hepatocyte PM flotillin 1 and FC content were normalized after the addition of 10% fetal bovine serum (FBS; 300 μg cholesterol per milliliter) to control hepatocyte levels (data not shown), demonstrating that acute repletion of HSKO hepatocyte PM cholesterol was possible with FBS-containing lipoproteins.

We performed a lipidomic analysis of PL species in chow-fed fl/fl and HSKO mouse livers. Hepatic content of phosphatidylcholine (PC), phosphatidylethanolamine (PE), phosphatidylinositol (PI), phosphatidylserine (PS), and phosphatidic acid (PA) were unaffected by ABCA1 expression (Figure S5D). However, lyso-PC, lyso-PE, and lysophatidylglycerol (lyso-PG) were significantly increased (1.9-, 1.5-, and 2.8-fold, respectively, $p < 0.01$) in HSKO liver versus fl/fl liver (Figure 5E). HSKO liver lyso-PC and lyso-PE species also contained less saturated and monounsaturated fatty acyl species versus polyunsaturated species (Figure 5F, Sat+Mono/Poly ratio), compared to fl/fl liver ($p < 0.05$), suggesting a selective remodeling of hepatic lyso-PL without ABCA1.

We also measured hepatocyte PM cholesterol and flotillin 1 content from WTD-fed mice. Compared to chow-fed mice (Figure 5C), PM fractions from WTD-fed mice were likely contaminated with lipid droplets based on perilipin 2 content (Figure 5G). Regardless, PM flotillin 1 (Figure 5G) and FC content (Figure 5H) were decreased by ~30% ($p < 0.001$) in primary hepatocytes isolated from WTD-fed HSKO mice versus controls.

To directly test effects of acute cholesterol depletion and repletion on insulin signaling, we treated hepatocytes from WTD-fed mice with methyl-β-cyclodextrin (MβCD) or cholesterol-loaded MβCD and then stimulated them acutely with insulin and measured Akt phosphorylation. MβCD-treated hepatocytes had no detectable Akt phosphorylation for both genotypes (Figure 5I) and reduced cellular FC content (Figure 5J). Incubation of MβCD-treated hepatocytes with cholesterol-loaded MβCD increased cellular FC and restored insulin-stimulated Akt phosphorylation, both above basal levels for both genotypes (Figures 5I and 5J), demonstrating that acute FC depletion and repletion

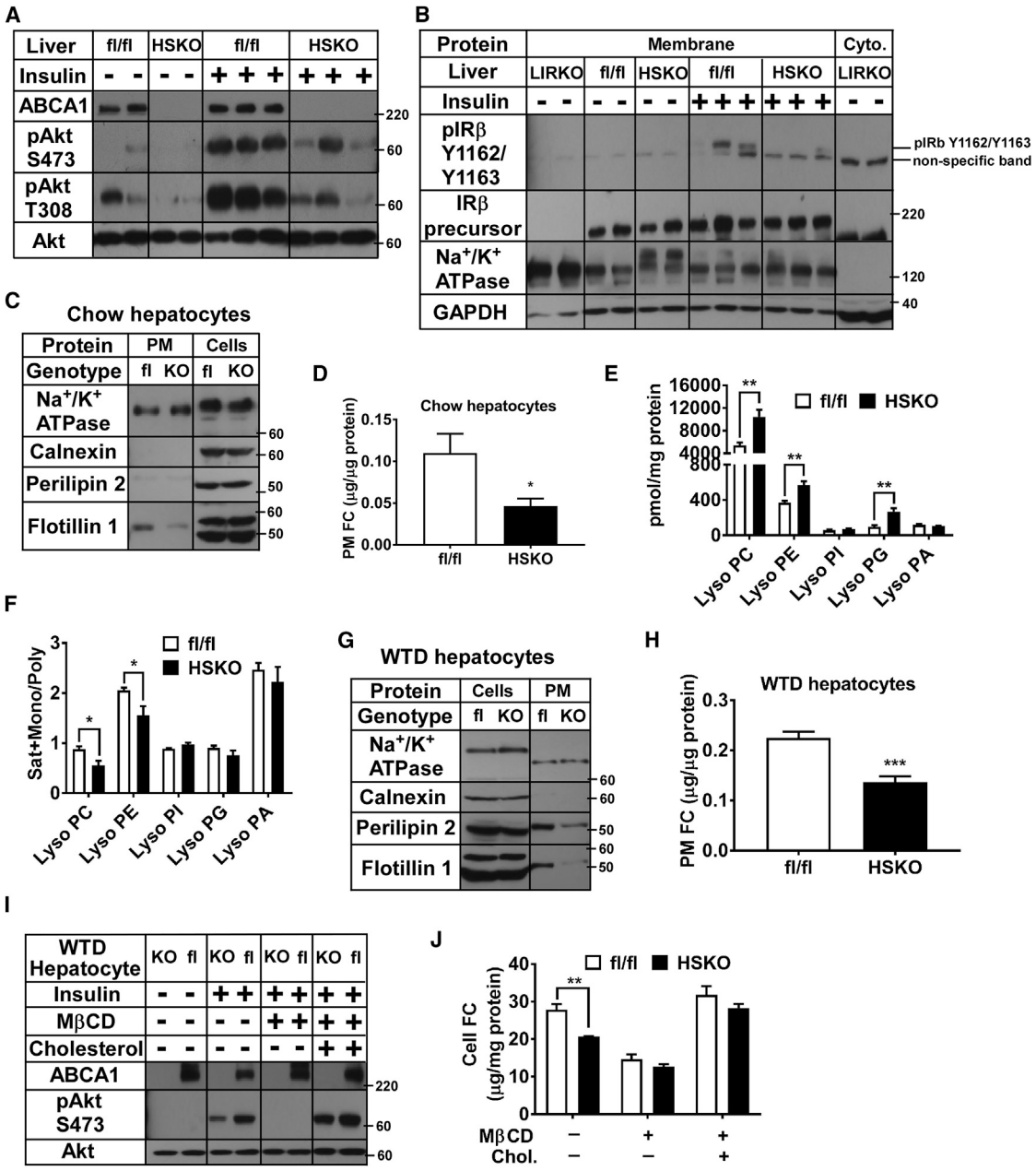

Figure 5. Primary Hepatocyte PM FC Content Modulates Insulin Signaling

Mice consuming a WTD for 16–24 weeks received a portal vein saline (n = 2 per genotype) or an insulin (0.5 U/kg of body weight; n = 3 per genotype) injection; 5 min later, livers were harvested.

(A) Liver western blots. p, phosphorylated.

(B) Western blots of hepatic membrane-associated and cytosolic (Cyto.) proteins. LIRKO, liver-specific insulin receptor knockout.

(C and D) Primary hepatocytes from chow-fed mice (n = 2 per genotype) were used to purify PM fractions (n = 3 per treatment) for western blot (C) and FC measures (D).

(E and F) Liver lipids were extracted from chow-fed mice (n = 4 per genotype) to measure lysophospholipid content (E) and fatty acyl species (F), which are shown as the ratio of saturated (Sat) + monosaturated (Mono) divided by polyunsaturated (Poly) fatty acyl chains.

(G and H) Primary hepatocytes from WTD-fed mice (n = 2 per genotype) were used to purify PM (n = 6 per treatment) for western blotting (G) and FC quantification (H).

(I) Primary hepatocytes from WTD-fed mice (n = 2 per genotype) were FC depleted (+MβCD) and repleted (+cholesterol) before insulin stimulation (n = 3 per treatment) and western blotting.

(J) Cells from (I) were lipid extracted and FC measured. Chol., cholesterol.

Results are representative of two to three separate experiments. *p < 0.05; **p < 0.01; ***p < 0.001. All results are mean ± SEM.

See also Figure S5.

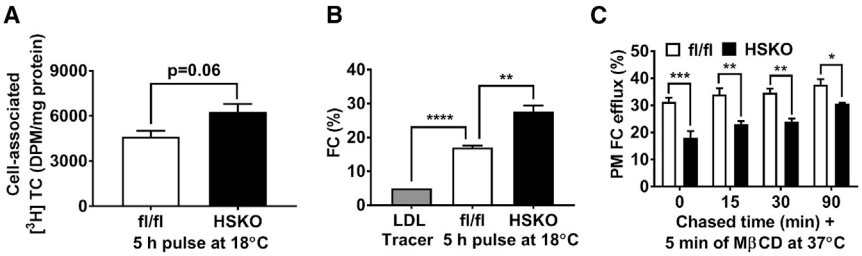

Figure 6. Defective Intracellular FC Trafficking in ABCA1-Deficient Hepatocytes

Hepatocytes (n = 3 per treatment) were isolated from chow-fed, male mice and incubated with [^{3}H]-cholesteryl-oleate-radiolabeled low-density lipoprotein (LDL) tracer for 5 hr at 18°C.

(A and B) After the 5-hr pulse, (A) cell-associated [^{3}H]-TC and (B) percent FC were quantified. DPM, disintegrations per minute.

(C) After incubation with LDL tracer, cells were chased for 0, 15, 30, and 90 min at 37°C and then treated with 3 mM MβCD for 5 min at 37°C to extract PM [^{3}H]-FC.

Results are representative of two separate experiments. *$p < 0.05$; **$p < 0.01$; ***$p < 0.001$; and ****$p < 0.0001$. All results are mean ± SEM.

resulted in decreased and increased insulin-stimulated signaling, respectively.

Hepatic *Abca1* Deletion Impairs Antegrade FC Trafficking from Lysosomes to the PM

Since we observed a significant decrease in HSKO hepatocyte PM FC content (Figure 5D)—but not total cellular FC level (Figure S1I)—compared to fl/fl controls, we hypothesized that intracellular cholesterol trafficking is defective in ABCA1-deficient hepatocytes. Because LDL trafficking from endosomes to lysosomes is blocked at 18°C (Jones, 1997; Sugii et al., 2003), we incubated primary hepatocytes isolated from chow-fed mice with [^{3}H]-cholesteryl-oleate-containing LDL at 18°C for 5 hr to pulse-label the endosomal compartment. Radiolabel was chased for 90 min at 37°C to allow LDL trafficking to the lysosome and hydrolysis of LDL [^{3}H]-cholesteryl oleate to [^{3}H]-FC and oleic acid. Cell-associated (bound + internalized) [^{3}H]-total (CE + FC) cholesterol trended higher ($p = 0.06$) in chow-fed HSKO versus fl/fl hepatocytes (Figure 6A) after the pulse period, possibly due to increased hepatic LDL receptor protein expression in HSKO liver (Chung et al., 2010). During the pulse period, some hydrolysis of LDL [^{3}H]-cholesteryl oleate occurred, detected as higher cell-associated FC radiolabel compared to the LDL tracer (5% FC; 95% CE) (Figure 6B); increased FC radiolabel was significantly higher in HSKO (28% FC) versus fl/fl (17% FC) hepatocytes (Figure 6B), likely reflecting the higher total cell-associated radiolabel in HSKO hepatocytes (Figure 6A). To monitor the arrival of [^{3}H]-FC at the PM during the chase period, hepatocytes were incubated with MβCD for 5 min at 37°C, followed by lipid extraction of cells and media and isolation of [^{3}H]-FC by thin-layer chromatography (Sugii et al., 2003). Despite more [^{3}H]-FC radiolabel in HSKO cells (Figure 6B), MβCD-extractable PM [^{3}H]-FC was lower for HSKO hepatocytes at zero time (42%, $p < 0.001$) and all three chase times (32%, $p < 0.01$; 31%, $p < 0.01$; and 20%, $p < 0.05$, respectively) relative to fl/fl hepatocytes (Figure 6C), suggesting impaired antegrade trafficking of lysosomal FC to the PM in HSKO hepatocytes.

DISCUSSION

Prior studies suggest that ABCA1 may be important in regulating systemic glucose metabolism and hepatic insulin signaling (Brunham et al., 2007; Chung et al., 2010; de Haan et al., 2014b), but mechanisms were unclear. A summary of our findings appears in Figure 7A. Compared to control (fl/fl) mice, HSKO mice had decreased hepatic insulin receptor signaling due to decreased PM FC content that likely resulted from defective antegrade lysosomal FC trafficking to the PM and decreased cholesterol biosynthesis. Decreased PM FC content and impaired PM signaling led to decreased mTORC activation; an ~50% reduction in SREBP1c mRNA abundance; decreased unprocessed, full-length SREBP1c; and low levels of processed nuclear SREBP1c, a critical transcriptional activator of de novo lipogenesis. Feeding a WTD to HSKO mice, compared to fl/fl controls, markedly decreased hepatic TG content, associated with decreased de novo lipogenesis and FA uptake and a mild metabolic phenotype (reduced body weight and increased energy expenditure). Nonetheless, hepatic and systemic glucose metabolism remained intact. Our results support the concept that hepatocyte ABCA1 is critical for maintaining optimal PM FC content for efficient membrane (particularly insulin) signaling. Without hepatocyte ABCA1, a unique form of insulin resistance is unmasked, where de novo lipogenesis is suppressed, but gluconeogenesis remains responsive (Figure 7B).

A striking result of our study was decreased hepatic insulin signaling and de novo lipogenesis in HSKO mice. Li et al. showed that insulin signaling bifurcates at the level of mTORC activation, with one pathway stimulating de novo lipogenesis and one inhibiting gluconeogenesis (Li et al., 2010). Akt-dependent lipogenesis requires mTORC activation (Porstmann et al., 2008). Our results show that components of the insulin signaling pathway proximal (PI3K [Chung et al., 2010] and Akt) and distal (S6K and 4E-BP1) to mTORC are attenuated in HSKO versus fl/fl liver. Decreased de novo lipogenesis in HSKO liver is supported by reduced SREBP1c mRNA, protein expression, and protein processing and by biochemical measurements. Decreased SREBP1c processing and lipogenesis in HSKO livers were most likely due to impaired insulin receptor activation resulting from reduced PM FC, since SREBP1c mRNA and full-length, unprocessed protein decreased in a manner proportional to that of processed nuclear SREBP1c. However, increased endoplasmic reticulum (ER) FC content, which would result in increased ER retention of SCAP-SREBP1c by INSIG (Engelking et al., 2004; Yabe et al., 2002), may be partially responsible for decreased de novo lipogenesis in HSKO liver.

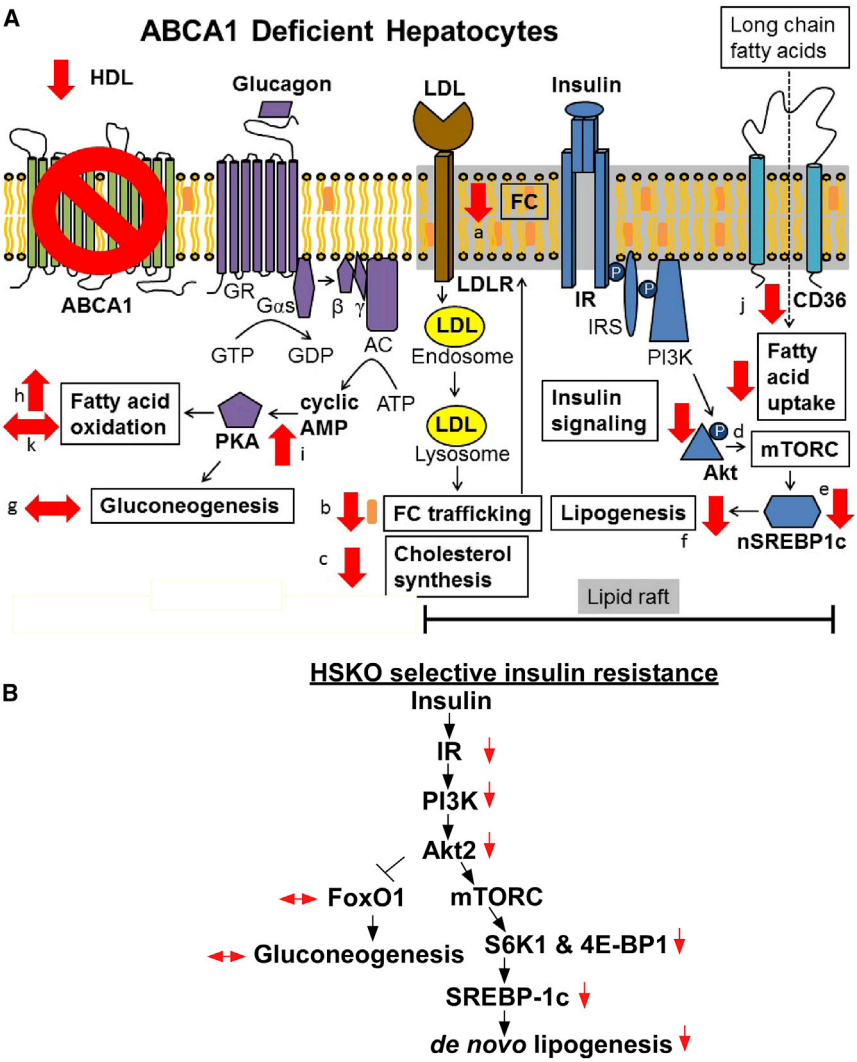

Figure 7. Summary of Experimental Results

(A) Compared to chow-fed control (fl/fl) mice, hepatic insulin signaling is reduced in chow-fed HSKO mice due to reduced PM FC content (a) from decreased trafficking of lysosomal FC to the PM (b) and cholesterol biosynthesis (c). Blunted insulin signaling leads to decreased activation of the Akt-mTORC pathway (d) and decreased expression and processing of SREBP1c (e), resulting in reduced de novo lipogenesis (f). Regulation of gluconeogenesis is unchanged in HSKO versus fl/fl liver (g), but FA oxidation is increased (h), perhaps due to the activation of glucagon signaling (i). WTD-fed HSKO mice, compared to control mice, have a similar phenotype with decreased PM FC (a), decreased insulin signaling (d), and reduced lipogenesis (f), resulting in diminished hepatosteatosis. However, unlike in chow-fed mice, the liver in WTD-fed HSKO mouse had decreased FA uptake (j; dashed arrow) and similar FA oxidation (k), compared to that in WTD-fed control mice. LDLR, LDL receptor; GR, glucagon receptor; AC, adenylate cyclase; IR, insulin receptor; IRS, insulin receptor substrate.

(B) Proposed sequence leading to unique selective insulin resistance in HSKO mouse liver. Downward arrows indicate decreased signal pathway/molecule activation relative to fl/fl (control) mice; horizontal arrows denote no change. The HSKO mouse liver shows a defect in the Akt2 and mTORC1 response to insulin, with a concomitant reduction in de novo lipogenesis. FoxO1 and gluconeogenesis remain suppressed by insulin.

HSKO mice subjected to fasting and refeeding appropriately downregulated gluconeogenic gene expression and nuclear FoxO1 and upregulated Gck, similar to control mice, resulting in no overt systemic abnormality in glucose regulation. In agreement with our results, other studies have shown that hepatic insulin signaling is dispensable for normal postprandial response of gluconeogenic genes but required for inducing lipogenesis through SREBP1c activation (Titchenell et al., 2015, 2016).

Although ABCA1 is critical for generating plasma HDL (Timmins et al., 2005), it is also involved in endocytosis (Zha et al., 2001), exocytosis (Kruit et al., 2011), intracellular vesicular trafficking (Robenek and Schmitz, 1991; Schmitz et al., 1985; Zha et al., 2003), and reducing membrane lipid rafts (Landry et al., 2006; Zarubica et al., 2009; Zhu et al., 2008, 2010). More recently, ABCA1 was implicated in retrograde transport of FC from PM to ER (Yamauchi et al., 2015) to regulate ER cholesterol content, a key step in controlling sterol biosynthesis (Radhakrishnan et al., 2008), and autonomous regulation of cellular membrane composition in response to cell crowding (Frechin et al., 2015). In the latter study, cultured cells with low crowding responded by downregulating ABCA1, resulting in higher cellular cholesterol content, more lipid droplets, and more saturated cell membrane PL species. A more rigid membrane structure results that affects membrane receptor signaling, such as Akt phosphorylation, which critically depends on membrane lipid raft domains for optimal activation (Lasserre et al., 2008). Frechin et al. (2015) postulate that the PM may act as a capacitor that converts signals to the correct timescale and is tuned by enzymes that alter membrane lipid composition and order. Our results with hepatocytes, and those of Frechin et al. using non-hepatic cells, demonstrate a generalizable and key role for ABCA1 in determining PM composition and order, which modulates cellular signaling (i.e., insulin and glucagon).

Using mouse embryonic fibroblasts from whole-body *Abca1* knockout mice, endocytic retrograde FC movement from the PM to the ER was impaired compared to that of WT mouse embryonic fibroblasts, which increased activation of the SREBP2 pathway and cholesterol biosynthesis (Yamauchi et al., 2015). Furthermore, these authors documented increased PM FC and lipid raft content (i.e., flotillin-1 and caveolin-1), the opposite of our findings in HSKO hepatocytes. We propose that ABCA1 is

more dominant in antegrade FC transport than in retrograde transport in hepatocytes, which are programmed to be secretory cells. Defective vesicular trafficking and antegrade movement of lipid occur in cells lacking ABCA1 (Robenek and Schmitz, 1991; Schmitz et al., 1985; Zha et al., 2003). Despite increased cell-associated [^{3}H]-FC in HSKO hepatocytes, movement of lysosomal [^{3}H]-FC cholesterol, liberated by the hydrolysis of LDL [^{3}H]-CE, to the PM, is impaired in ABCA1-deficient hepatocytes. With reduced intracellular FC trafficking to the PM, ER FC may increase, leading to the downregulation of FC and TG synthesis, by decreasing SREBP1c processing and nuclear SREBP1c content (Nohturfft et al., 2000; Wang et al., 1994), as supported by our results (Figure 2H). Thus, the role of ABCA1 in antegrade and retrograde FC transport may be cell specific and dictated by the overall need to take up or secrete lipid.

Mice completely lacking hepatocyte insulin receptors (i.e., LIRKO) are hyperinsulinemic, with mildly elevated blood glucose, but plasma TG concentrations are lower than in controls (Biddinger et al., 2008). The pure insulin resistance in LIRKO mice results in decreased de novo lipogenesis due to decreased SREBP1c activation (Haas et al., 2012), unlike the selective insulin resistance observed in mouse models of obesity/type 2 diabetes (i.e., *ob/ob*) or mice fed a WTD, both of which have increased de novo lipogenesis, hepatosteatosis, and hypertriglyceridemia (Brown and Goldstein, 2008). Chow-fed HSKO mice have some phenotypic features of LIRKO mice (Biddinger et al., 2008; Haas et al., 2012), including elevated plasma glucose concentrations (Figure S1J) and lower fasting plasma TG concentrations (Chung et al., 2010). When challenged with a HFD, both LIRKO (Haas et al., 2012) and HSKO mice (Figure 3) had decreased body weight gain and were relatively protected from hepatosteatosis, compared to control mice. However, unlike LIRKO mice, HSKO mice were not hyperinsulinemic (Figure S1K), likely due to normal plasma insulin clearance by hepatocyte insulin receptors and normal pancreatic insulin secretion without significantly elevated plasma glucose levels. Insulin signaling strongly activates lipogenesis by increasing SREBP1c mRNA abundance and protein processing (Jeon and Osborne, 2012). Chow-fed LIRKO and HSKO mice have reduced SREBP1c expression and processing, compared to their respective controls, when refed a high-carbohydrate chow diet after a prolonged fast. These similarities suggest that HSKO mice exhibit a phenotype more similar to pure insulin resistance than selective insulin resistance (Brown and Goldstein, 2008). If defective lysosomal FC trafficking to the PM reroutes FC trafficking to the ER, as suggested by our RNA-seq and in vitro cholesterol biogenesis data, then SREBP1c processing may be further attenuated by ER INSIG-mediated retention of the SCAP-SREBP1c complex (Engelking et al., 2004; Yabe et al., 2003).

EXPERIMENTAL PROCEDURES

Mice

HSKO mice were generated by crossing fl/fl mice (Timmins et al., 2005) (backcrossed into the >99% C57BL/6 background) with albumin *Cre* recombinase transgenic mice (Jackson Laboratory). Age-matched (8–24 weeks of age) male mice on chow (LabDiet 5P00 Prolab RMH 3000) or a WTD were used. Eight-week-old chow-fed male mice were switched to WTD (42% fat calories, 0.2% cholesterol; Harlan Laboratories TD88137) for 16–24 weeks to induce obesity, insulin resistance, and hepatic steatosis. All mice were maintained in a specific pathogen-free environment on a 12-hr:12-hr light:dark cycle (dark from 6 p.m. to 6 a.m.) and allowed free access to food and water. All experiments were performed using a protocol approved by the Institutional Animal Care and Use Committee at Wake Forest School of Medicine in facilities approved by the American Association for Accreditation of Laboratory Animal Care.

For the fasting/refeeding study, chow-fed mice (n = 3 per genotype) were fasted for 24 hr (6 a.m. to 6 a.m.), and another group was fasted for 24 hr (10 p.m. to 10 p.m.) followed by refeeding a high-carbohydrate chow (LabDiet 5P00 Prolab RMH 3000) for 8 hr (10 p.m. to 6 a.m.). All mice were terminated between 6 a.m. and 7 a.m. Fresh liver (~200 mg) was used to isolate nuclear protein to examine SREBP1 expression (Bennett et al., 2008). The remainder was immediately frozen in liquid nitrogen and stored at −80°C until proteins were isolated and RNA was extracted for western blotting and real-time PCR, respectively.

Indirect Calorimetry

Indirect calorimetry was conducted as described previously (Thomas et al., 2013). Food intake was independently verified over 14 days, using mice housed in individual wire-bottom cages (Thomas et al., 2013).

Metabolic Measurements

Metabolic measurements were conducted as described previously (Chung et al., 2010; Thomas et al., 2013), with slight modifications as detailed in the Supplemental Experimental Procedures.

In Vivo TG Secretion Rate

In vivo TG secretion was measured by a detergent lipolysis block procedure with radiolabeled oleic acid (Bi et al., 2013; Chung et al., 2010).

In Vivo Insulin Signaling Analysis

Liver, adipose tissue, and muscle insulin signaling were determined as previously described (Chung et al., 2010) with slight modifications; see Supplemental Experimental Procedures.

RNA-Seq and Real-Time PCR

RNA-seq and real-time PCR were performed as described in the Supplemental Experimental Procedures.

Western Blotting

Western blots were performed after protein fractionation using SDS-PAGE (Chung et al., 2010). Antibodies used for western blots are listed in the Supplemental Experimental Procedures.

In Vitro Metabolic Analyses

Primary hepatocytes were isolated as described in the Supplemental Experimental Procedures (Kreamer et al., 1986). Hepatic insulin signaling (Zhu et al., 2010), glucagon signaling (Miller et al., 2013), lipogenesis (Thomas et al., 2013), FA uptake (Li et al., 2013), and FA oxidation (Huynh et al., 2014) were analyzed using methods described in the Supplemental Experimental Procedures.

Lipid Analysis of PM Fraction Isolated from Primary Hepatocytes

Primary hepatocyte PM isolation was performed as previously described (Das et al., 2013, 2014); see the Supplemental Experimental Procedures.

Intracellular Cholesterol Trafficking

Trafficking of lysosomal FC to the PM was measured as described in the Supplemental Experimental Procedures (Sugii et al., 2003).

Lipidomic Analyses

Liver lipids were extracted from chow-fed mice (Folch et al., 1957) for mass spectrometry quantification of lyso-PL (Bollinger et al., 2010) and PL head group and fatty acyl species (Sorci-Thomas et al., 2012); see the Supplemental Experimental Procedures.

Immunofluorescence

Immunofluorescent staining was performed as described in the Supplemental Experimental Procedures (Tamura and Yui, 2014).

Statistics

Results are presented as mean ± SEM. Data were analyzed using an unpaired two-tailed Student's t test, one-way ANOVA with Tukey's multiple comparison test, or two-way ANOVA with Bonferroni's multiple comparison test. When unequal variance among groups was present, data were log-transformed before performing ANOVA. All analyses were performed using GraphPad Prism 7 software. Significant differences are denoted as follows: *$p < 0.05$, **$p < 0.01$, ***$p < 0.001$, and ****$p < 0.0001$; for multiple comparisons, different lowercase letters denote significant differences ($p < 0.05$; Figure 2).

ACCESSION NUMBERS

The accession number for the RNA-seq files reported in this paper is GEO: GSE96093.

SUPPLEMENTAL INFORMATION

Supplemental Information includes Supplemental Experimental Procedures, five figures, and four tables and can be found with this article online at http://dx.doi.org/10.1016/j.celrep.2017.05.032.

AUTHOR CONTRIBUTIONS

C.-C.C.K. designed and performed all the experiments and analysis, except the RNA-seq study, and wrote the manuscript. M.L. assisted with indirect calorimetry, in vivo insulin signaling analysis, and primary hepatocyte isolation, conducted the experiment of in vivo determination of TG secretion, and generated preliminary data. C.L.K. performed real-time PCR experiments and analysis and assisted with RNA-seq analysis. S.C. initiated the project and generated preliminary data. E.B. assisted with real-time PCR analysis. T.A.D. assisted with RNA-seq analysis. A.B. prepared [^{3}H]-cholesteryl-oleate-radiolabeled low-density lipoproteins. P.E.P. assisted in studying SREBP processing. B.I.F. assisted in immunofluorescence experiments and manuscript editing. T.F.O. provided SREBP1 antibody and assisted in studying SREBP processing. X.Z. assisted in measuring cholesterol and lipid raft content. L.M. performed immunofluorescence experiments. P.S. designed RNA-seq experiments and performed analysis. S.B.B. provided liver samples of liver-specific insulin receptor knockout mice, assisted in studying insulin signaling, and edited the manuscript. J.S.P. designed all the experiments except the RNA-seq study and wrote the manuscript.

ACKNOWLEDGMENTS

This work was supported by NIH grants HL119962 (to J.S.P.), DK105965 (to P.S.), HL48044 (to T.F.O.), and HL109650 (to S.B.B.). We gratefully acknowledge services provided by (1) the Lipid, Lipoprotein and Atherosclerosis Analysis Laboratory of the Department of Internal Medicine/Section on Molecular Medicine; (2) the Proteomics and Metabolomics Shared Resource; and (3) the Cell and Viral Vector Core Laboratory (supported in part by NCI P30 CA121291-37) of the Comprehensive Cancer Center at the Wake Forest School of Medicine. We also acknowledge the editorial assistance of Karen Klein, MA, in the Wake Forest Clinical and Translational Science Institute (project no. UL1 TR001420; PI: Donald McClain).

Received: September 14, 2016
Revised: March 7, 2017
Accepted: May 9, 2017
Published: June 6, 2017

REFERENCES

Adiels, M., Borén, J., Caslake, M.J., Stewart, P., Soro, A., Westerbacka, J., Wennberg, B., Olofsson, S.O., Packard, C., and Taskinen, M.R. (2005). Overproduction of VLDL1 driven by hyperglycemia is a dominant feature of diabetic dyslipidemia. Arterioscler. Thromb. Vasc. Biol. *25*, 1697–1703.

Bennett, M.K., Seo, Y.K., Datta, S., Shin, D.J., and Osborne, T.F. (2008). Selective binding of sterol regulatory element-binding protein isoforms and co-regulatory proteins to promoters for lipid metabolic genes in liver. J. Biol. Chem. *283*, 15628–15637.

Bi, X., Zhu, X., Duong, M., Boudyguina, E.Y., Wilson, M.D., Gebre, A.K., and Parks, J.S. (2013). Liver ABCA1 deletion in LDLrKO mice does not impair macrophage reverse cholesterol transport or exacerbate atherogenesis. Arterioscler. Thromb. Vasc. Biol. *33*, 2288–2296.

Bickel, P.E. (2002). Lipid rafts and insulin signaling. Am. J. Physiol. Endocrinol. Metab. *282*, E1–E10.

Bickel, P.E., Scherer, P.E., Schnitzer, J.E., Oh, P., Lisanti, M.P., and Lodish, H.F. (1997). Flotillin and epidermal surface antigen define a new family of caveolae-associated integral membrane proteins. J. Biol. Chem. *272*, 13793–13802.

Biddinger, S.B., and Kahn, C.R. (2006). From mice to men: insights into the insulin resistance syndromes. Annu. Rev. Physiol. *68*, 123–158.

Biddinger, S.B., Hernandez-Ono, A., Rask-Madsen, C., Haas, J.T., Alemán, J.O., Suzuki, R., Scapa, E.F., Agarwal, C., Carey, M.C., Stephanopoulos, G., et al. (2008). Hepatic insulin resistance is sufficient to produce dyslipidemia and susceptibility to atherosclerosis. Cell Metab. *7*, 125–134.

Bollinger, J.G., Ii, H., Sadilek, M., and Gelb, M.H. (2010). Improved method for the quantification of lysophospholipids including enol ether species by liquid chromatography-tandem mass spectrometry. J. Lipid Res. *51*, 440–447.

Brown, M.S., and Goldstein, J.L. (2008). Selective versus total insulin resistance: a pathogenic paradox. Cell Metab. *7*, 95–96.

Brunham, L.R., Kruit, J.K., Pape, T.D., Timmins, J.M., Reuwer, A.Q., Vasanji, Z., Marsh, B.J., Rodrigues, B., Johnson, J.D., Parks, J.S., et al. (2007). Beta-cell ABCA1 influences insulin secretion, glucose homeostasis and response to thiazolidinedione treatment. Nat. Med. *13*, 340–347.

Campbell, J.E., and Drucker, D.J. (2015). Islet α cells and glucagon–critical regulators of energy homeostasis. Nat. Rev. Endocrinol. *11*, 329–338.

Cheng, Z., and White, M.F. (2012). kNOXing on the door of selective insulin resistance. Arterioscler. Thromb. Vasc. Biol. *32*, 1063–1065.

Chung, S., Timmins, J.M., Duong, M., Degirolamo, C., Rong, S., Sawyer, J.K., Singaraja, R.R., Hayden, M.R., Maeda, N., Rudel, L.L., et al. (2010). Targeted deletion of hepatocyte ABCA1 leads to very low density lipoprotein triglyceride overproduction and low density lipoprotein hypercatabolism. J. Biol. Chem. *285*, 12197–12209.

Daimon, M., Kido, T., Baba, M., Oizumi, T., Jimbu, Y., Kameda, W., Yamaguchi, H., Ohnuma, H., Tominaga, M., Muramatsu, M., and Kato, T. (2005). Association of the ABCA1 gene polymorphisms with type 2 DM in a Japanese population. Biochem. Biophys. Res. Commun. *329*, 205–210.

Das, A., Goldstein, J.L., Anderson, D.D., Brown, M.S., and Radhakrishnan, A. (2013). Use of mutant 125I-perfringolysin O to probe transport and organization of cholesterol in membranes of animal cells. Proc. Natl. Acad. Sci. USA *110*, 10580–10585.

Das, A., Brown, M.S., Anderson, D.D., Goldstein, J.L., and Radhakrishnan, A. (2014). Three pools of plasma membrane cholesterol and their relation to cholesterol homeostasis. eLife *3*, e02882.

de Haan, W., Bhattacharjee, A., Ruddle, P., Kang, M.H., and Hayden, M.R. (2014a). ABCA1 in adipocytes regulates adipose tissue lipid content, glucose tolerance, and insulin sensitivity. J. Lipid Res. *55*, 516–523.

de Haan, W., Karasinska, J.M., Ruddle, P., and Hayden, M.R. (2014b). Hepatic ABCA1 expression improves β-cell function and glucose tolerance. Diabetes *63*, 4076–4082.

Engelking, L.J., Kuriyama, H., Hammer, R.E., Horton, J.D., Brown, M.S., Goldstein, J.L., and Liang, G. (2004). Overexpression of Insig-1 in the livers of transgenic mice inhibits SREBP processing and reduces insulin-stimulated lipogenesis. J. Clin. Invest. *113*, 1168–1175.

Folch, J., Lees, M., and Sloane Stanley, G.H. (1957). A simple method for the isolation and purification of total lipides from animal tissues. J. Biol. Chem. *226*, 497–509.

Frechin, M., Stoeger, T., Daetwyler, S., Gehin, C., Battich, N., Damm, E.M., Stergiou, L., Riezman, H., and Pelkmans, L. (2015). Cell-intrinsic adaptation of lipid composition to local crowding drives social behaviour. Nature *523*, 88–91.

Goldstein, J.L., and Brown, M.S. (2015). A century of cholesterol and coronaries: from plaques to genes to statins. Cell *161*, 161–172.

Haas, J.T., Miao, J., Chanda, D., Wang, Y., Zhao, E., Haas, M.E., Hirschey, M., Vaitheesvaran, B., Farese, R.V., Jr., Kurland, I.J., et al. (2012). Hepatic insulin signaling is required for obesity-dependent expression of SREBP-1c mRNA but not for feeding-dependent expression. Cell Metab. *15*, 873–884.

Horton, J.D., Bashmakov, Y., Shimomura, I., and Shimano, H. (1998). Regulation of sterol regulatory element binding proteins in livers of fasted and refed mice. Proc. Natl. Acad. Sci. USA *95*, 5987–5992.

Huynh, F.K., Green, M.F., Koves, T.R., and Hirschey, M.D. (2014). Measurement of fatty acid oxidation rates in animal tissues and cell lines. Methods Enzymol. *542*, 391–405.

Ito, A., Hong, C., Rong, X., Zhu, X., Tarling, E.J., Hedde, P.N., Gratton, E., Parks, J., and Tontonoz, P. (2015). LXRs link metabolism to inflammation through Abca1-dependent regulation of membrane composition and TLR signaling. eLife *4*, e08009.

Jeon, T.I., and Osborne, T.F. (2012). SREBPs: metabolic integrators in physiology and metabolism. Trends Endocrinol. Metab. *23*, 65–72.

Jones, N.L. (1997). Simultaneous labeling of lipoprotein intracellular trafficking in pigeon monocyte-derived macrophages. Am. J. Pathol. *150*, 1113–1124.

Kreamer, B.L., Staecker, J.L., Sawada, N., Sattler, G.L., Hsia, M.T., and Pitot, H.C. (1986). Use of a low-speed, iso-density percoll centrifugation method to increase the viability of isolated rat hepatocyte preparations. In Vitro Cell. Dev. Biol. *22*, 201–211.

Kruit, J.K., Wijesekara, N., Fox, J.E., Dai, X.Q., Brunham, L.R., Searle, G.J., Morgan, G.P., Costin, A.J., Tang, R., Bhattacharjee, A., et al. (2011). Islet cholesterol accumulation due to loss of ABCA1 leads to impaired exocytosis of insulin granules. Diabetes *60*, 3186–3196.

Landry, Y.D., Denis, M., Nandi, S., Bell, S., Vaughan, A.M., and Zha, X. (2006). ATP-binding cassette transporter A1 expression disrupts raft membrane microdomains through its ATPase-related functions. J. Biol. Chem. *281*, 36091–36101.

Lasserre, R., Guo, X.J., Conchonaud, F., Hamon, Y., Hawchar, O., Bernard, A.M., Soudja, S.M., Lenne, P.F., Rigneault, H., Olive, D., et al. (2008). Raft nanodomains contribute to Akt/PKB plasma membrane recruitment and activation. Nat. Chem. Biol. *4*, 538–547.

Leavens, K.F., and Birnbaum, M.J. (2011). Insulin signaling to hepatic lipid metabolism in health and disease. Crit. Rev. Biochem. Mol. Biol. *46*, 200–215.

Li, S., Brown, M.S., and Goldstein, J.L. (2010). Bifurcation of insulin signaling pathway in rat liver: mTORC1 required for stimulation of lipogenesis, but not inhibition of gluconeogenesis. Proc. Natl. Acad. Sci. USA *107*, 3441–3446.

Li, Y., Dong, J., Ding, T., Kuo, M.S., Cao, G., Jiang, X.C., and Li, Z. (2013). Sphingomyelin synthase 2 activity and liver steatosis: an effect of ceramide-mediated peroxisome proliferator-activated receptor γ2 suppression. Arterioscler. Thromb. Vasc. Biol. *33*, 1513–1520.

Miller, R.A., Chu, Q., Xie, J., Foretz, M., Viollet, B., and Birnbaum, M.J. (2013). Biguanides suppress hepatic glucagon signalling by decreasing production of cyclic AMP. Nature *494*, 256–260.

Murphy, A.J., Akhtari, M., Tolani, S., Pagler, T., Bijl, N., Kuo, C.L., Wang, M., Sanson, M., Abramowicz, S., Welch, C., et al. (2011). ApoE regulates hematopoietic stem cell proliferation, monocytosis, and monocyte accumulation in atherosclerotic lesions in mice. J. Clin. Invest. *121*, 4138–4149.

Nohturfft, A., Yabe, D., Goldstein, J.L., Brown, M.S., and Espenshade, P.J. (2000). Regulated step in cholesterol feedback localized to budding of SCAP from ER membranes. Cell *102*, 315–323.

Oram, J.F., and Vaughan, A.M. (2006). ATP-binding cassette cholesterol transporters and cardiovascular disease. Circ. Res. *99*, 1031–1043.

Porchay, I., Péan, F., Bellili, N., Royer, B., Cogneau, J., Chesnier, M.C., Caradec, A., Tichet, J., Balkau, B., Marre, M., and Fumeron, F. (2006). ABCA1 single nucleotide polymorphisms on high-density lipoprotein-cholesterol and overweight: the D.E.S.I.R. study. Obesity (Silver Spring) *14*, 1874–1879.

Porstmann, T., Santos, C.R., Griffiths, B., Cully, M., Wu, M., Leevers, S., Griffiths, J.R., Chung, Y.L., and Schulze, A. (2008). SREBP activity is regulated by mTORC1 and contributes to Akt-dependent cell growth. Cell Metab. *8*, 224–236.

Radhakrishnan, A., Goldstein, J.L., McDonald, J.G., and Brown, M.S. (2008). Switch-like control of SREBP-2 transport triggered by small changes in ER cholesterol: a delicate balance. Cell Metab. *8*, 512–521.

Robenek, H., and Schmitz, G. (1991). Abnormal processing of Golgi elements and lysosomes in Tangier disease. Arterioscler. Thromb. *11*, 1007–1020.

Saltiel, A.R., and Kahn, C.R. (2001). Insulin signalling and the regulation of glucose and lipid metabolism. Nature *414*, 799–806.

Schmitz, G., Assmann, G., Robenek, H., and Brennhausen, B. (1985). Tangier disease: a disorder of intracellular membrane traffic. Proc. Natl. Acad. Sci. USA *82*, 6305–6309.

Simons, K., and Toomre, D. (2000). Lipid rafts and signal transduction. Nat. Rev. Mol. Cell Biol. *1*, 31–39.

Sorci-Thomas, M.G., Owen, J.S., Fulp, B., Bhat, S., Zhu, X., Parks, J.S., Shah, D., Jerome, W.G., Gerelus, M., Zabalawi, M., and Thomas, M.J. (2012). Nascent high density lipoproteins formed by ABCA1 resemble lipid rafts and are structurally organized by three apoA-I monomers. J. Lipid Res. *53*, 1890–1909.

Sugii, S., Reid, P.C., Ohgami, N., Du, H., and Chang, T.Y. (2003). Distinct endosomal compartments in early trafficking of low density lipoprotein-derived cholesterol. J. Biol. Chem. *278*, 27180–27189.

Tamura, A., and Yui, N. (2014). Lysosomal-specific cholesterol reduction by biocleavable polyrotaxanes for ameliorating Niemann-Pick type C disease. Sci. Rep. *4*, 4356.

Thomas, G., Betters, J.L., Lord, C.C., Brown, A.L., Marshall, S., Ferguson, D., Sawyer, J., Davis, M.A., Melchior, J.T., Blume, L.C., et al. (2013). The serine hydrolase ABHD6 is a critical regulator of the metabolic syndrome. Cell Rep. *5*, 508–520.

Timmins, J.M., Lee, J.Y., Boudyguina, E., Kluckman, K.D., Brunham, L.R., Mulya, A., Gebre, A.K., Coutinho, J.M., Colvin, P.L., Smith, T.L., et al. (2005). Targeted inactivation of hepatic Abca1 causes profound hypoalphalipoproteinemia and kidney hypercatabolism of apoA-I. J. Clin. Invest. *115*, 1333–1342.

Titchenell, P.M., Chu, Q., Monks, B.R., and Birnbaum, M.J. (2015). Hepatic insulin signalling is dispensable for suppression of glucose output by insulin in vivo. Nat. Commun. *6*, 7078.

Titchenell, P.M., Quinn, W.J., Lu, M., Chu, Q., Lu, W., Li, C., Chen, H., Monks, B.R., Chen, J., Rabinowitz, J.D., and Birnbaum, M.J. (2016). Direct hepatocyte insulin signaling is required for lipogenesis but is dispensable for the suppression of glucose production. Cell Metab. *23*, 1154–1166.

Vainio, S., Heino, S., Mansson, J.E., Fredman, P., Kuismanen, E., Vaarala, O., and Ikonen, E. (2002). Dynamic association of human insulin receptor with lipid rafts in cells lacking caveolae. EMBO Rep. *3*, 95–100.

Vainio, S., Bykov, I., Hermansson, M., Jokitalo, E., Somerharju, P., and Ikonen, E. (2005). Defective insulin receptor activation and altered lipid rafts in Niemann-Pick type C disease hepatocytes. Biochem. J. *391*, 465–472.

Villarreal-Molina, M.T., Aguilar-Salinas, C.A., Rodríguez-Cruz, M., Riaño, D., Villalobos-Comparan, M., Coral-Vazquez, R., Menjivar, M., Yescas-Gomez, P., Königsoerg-Fainstein, M., Romero-Hidalgo, S., et al.; Metabolic Study Group (2007). The ATP-binding cassette transporter A1 R230C variant affects HDL cholesterol levels and BMI in the Mexican population: association with obesity and obesity-related comorbidities. Diabetes *56*, 1881–1887.

Villarreal-Molina, M.T., Flores-Dorantes, M.T., Arellano-Campos, O., Villalobos-Comparan, M., Rodríguez-Cruz, M., Miliar-García, A., Huertas-Vazquez, A., Menjivar, M., Romero-Hidalgo, S., Wacher, N.H., et al.; Metabolic Study

Group (2008). Association of the ATP-binding cassette transporter A1 R230C variant with early-onset type 2 diabetes in a Mexican population. Diabetes *57*, 509–513.

Wang, X., Sato, R., Brown, M.S., Hua, X., and Goldstein, J.L. (1994). SREBP-1, a membrane-bound transcription factor released by sterol-regulated proteolysis. Cell *77*, 53–62.

Wu, X., and Williams, K.J. (2012). NOX4 pathway as a source of selective insulin resistance and responsiveness. Arterioscler. Thromb. Vasc. Biol. *32*, 1236–1245.

Yabe, D., Brown, M.S., and Goldstein, J.L. (2002). Insig-2, a second endoplasmic reticulum protein that binds SCAP and blocks export of sterol regulatory element-binding proteins. Proc. Natl. Acad. Sci. USA *99*, 12753–12758.

Yabe, D., Komuro, R., Liang, G., Goldstein, J.L., and Brown, M.S. (2003). Liver-specific mRNA for Insig-2 down-regulated by insulin: implications for fatty acid synthesis. Proc. Natl. Acad. Sci. USA *100*, 3155–3160.

Yamauchi, Y., Iwamoto, N., Rogers, M.A., Abe-Dohmae, S., Fujimoto, T., Chang, C.C.Y., Ishigami, M., Kishimoto, T., Kobayashi, T., Ueda, K., et al. (2015). Deficiency in the lipid exporter ABCA1 impairs retrograde sterol movement and disrupts sterol sensing at the endoplasmic reticulum. J. Biol. Chem. *290*, 23464–23477.

Yvan-Charvet, L., Pagler, T., Gautier, E.L., Avagyan, S., Siry, R.L., Han, S., Welch, C.L., Wang, N., Randolph, G.J., Snoeck, H.W., and Tall, A.R. (2010). ATP-binding cassette transporters and HDL suppress hematopoietic stem cell proliferation. Science *328*, 1689–1693.

Zarubica, A., Plazzo, A.P., Stöckl, M., Trombik, T., Hamon, Y., Müller, P., Pomorski, T., Herrmann, A., and Chimini, G. (2009). Functional implications of the influence of ABCA1 on lipid microenvironment at the plasma membrane: a biophysical study. FASEB J. *23*, 1775–1785.

Zha, X., Genest, J., Jr., and McPherson, R. (2001). Endocytosis is enhanced in Tangier fibroblasts: possible role of ATP-binding cassette protein A1 in endosomal vesicular transport. J. Biol. Chem. *276*, 39476–39483.

Zha, X., Gauthier, A., Genest, J., and McPherson, R. (2003). Secretory vesicular transport from the Golgi is altered during ATP-binding cassette protein A1 (ABCA1)-mediated cholesterol efflux. J. Biol. Chem. *278*, 10002–10005.

Zhu, X., Lee, J.Y., Timmins, J.M., Brown, J.M., Boudyguina, E., Mulya, A., Gebre, A.K., Willingham, M.C., Hiltbold, E.M., Mishra, N., et al. (2008). Increased cellular free cholesterol in macrophage-specific Abca1 knock-out mice enhances pro-inflammatory response of macrophages. J. Biol. Chem. *283*, 22930–22941.

Zhu, X., Owen, J.S., Wilson, M.D., Li, H., Griffiths, G.L., Thomas, M.J., Hiltbold, E.M., Fessler, M.B., and Parks, J.S. (2010). Macrophage ABCA1 reduces MyD88-dependent Toll-like receptor trafficking to lipid rafts by reduction of lipid raft cholesterol. J. Lipid Res. *51*, 3196–3206.

Zhu, X., Westcott, M.M., Bi, X., Liu, M., Gowdy, K.M., Seo, J., Cao, Q., Gebre, A.K., Fessler, M.B., Hiltbold, E.M., and Parks, J.S. (2012). Myeloid cell-specific ABCA1 deletion protects mice from bacterial infection. Circ. Res. *111*, 1398–1409.